Hindawi
Journal of Robotics
Volume 2017, Article ID 9467458, 8 pages
https://doi.org/10.1155/2017/9467458

Research Article

Concept Design and Analysis of a Novel Steamer-Filling Robot

Enhong Xing,[1] Bin Li,[1,2] and Xinhua Zhao[1]

[1]*Tianjin Key Laboratory for Advanced Mechatronic System Design and Intelligent Control, School of Mechanical Engineering, Tianjin University of Technology, Tianjin 300384, China*
[2]*National Demonstration Center for Experimental Mechanical and Electrical Engineering Education, Tianjin University of Technology, Tianjin, China*

Correspondence should be addressed to Bin Li; cnrobot@163.com

Received 30 July 2017; Revised 1 October 2017; Accepted 10 October 2017; Published 28 December 2017

Academic Editor: Gordon R. Pennock

Steamer-filling operation is a crucially important process in the liquor-making process, directly related to liquor yield and liquor quality. But so far, this process is still dominated by manual operation. In view of working environment and labor shortages in this industry, a novel exclusive steamer-filling robot is proposed in this paper. Firstly, the steamer-filling operation process is described, and the structure composition and function realization of the robot are particularly introduced. Secondly, the kinematics problems in terms of position analysis and workspace of the robot are analyzed in detail. Thirdly, experimental analyses are made to prove the validity and efficiency of the robot system. Finally, some conclusions and the future developing direction are prescribed.

1. Introduction

Liquor-making industry is a very important industry in China at present. According to the statistics, Chinese liquor production reached 960 million liters in 2015. Compared with automobile industry, electronics industry, food industry, and so on, the liquor-making industry is still dominated by manual operation. With growing shortage of labors and increasing labor costs, the demands on the automation equipment for liquor-making process are increasing, and these demands will generate a very large market.

Recently, a large number of wineries upgrade their automation equipment for steamer-filling operation. These technical methods can be divided into two categories, namely, nonrobot method and robot method [1–4]. For the nonrobot method, some conventional conveying devices, such as conveyor belt, are used to fill fermenting grains into fermentation containers. Since this method cannot fill fermenting grains in an automatic and well-distributed way, a worker is necessary, as shown in Figure 1; in other words, nonrobot method is just a semiautomatic method. The other method is robot method; in this way, the work system is composed of a six-degree-of-freedom manipulator and a hopper, which is fixed on the end of the manipulator. The working procedure is that, firstly, fermenting grains are filled in the hopper; then the manipulator is applied to simulate manual operation to toss fermenting grains into fermentation containers, as shown in Figure 2. Compared with the nonrobot method, this method can realize full automation, which is of vital significance to the liquor-making industry.

In this paper, a novel exclusive steamer-filling robot is proposed. Firstly, the steamer-filling operation process is described, and the structure composition and function realization of the robot are particularly introduced in Section 2. Secondly, the kinematics problems in terms of position analysis and workspace of the robot are analyzed in detail in Section 3. Thirdly, numerical experimental analyses are made to prove the validity and efficiency of the robot system in Section 4. The dynamic analysis of the robot is carried out in Section 5. Then the static stiffness of the robot is described in Section 6. Finally, some conclusions and the future developing direction are prescribed in Section 7.

2. Concept Design of Steamer-Filling Robot

In order to design the structure of the steamer-filling robot, it is necessary to introduce to the steamer-filling operation process. In general, steamer-filling operation means sprinkling

Figure 1: Nonrobot method for steamer-filling.

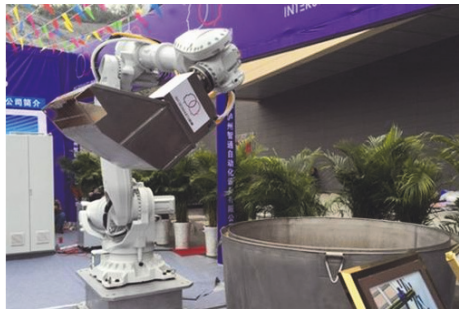

Figure 2: Robot method for steamer-filling.

fermenting grains into fermentation containers. In order to maximize liquor yield and liquor quality, the sprinkling process needs some skill requirements, such that operating should be quick, the fermenting grains should be porous, and the steamer should be well-distributed. For most wineries, the fermentation containers have a diameter of 2 meters and a height of 1.3 meters. A liquor worker should fill up a fermentation container within thirty-five minutes, which means hard-manual labor.

As mentioned above, a robot method has been proposed for steamer-filling operation to replace liquor workers. For this method, fermenting grains are filled in the hopper, which is fixed on the end of the robot; then the manipulator is applied to simulate manual operation to toss fermenting grains into fermentation containers. Through actual working experience, these existing steamer-filling robots have several downsides: for example, fermenting grains throwing process is a discontinuous process, which has important impact on production efficiency; fermenting grains throwing is not sufficiently homogeneous, which has an adverse effect on liquor yield and liquor quality.

Focusing on these problems of these already existing steamer-filling robots, a novel exclusive steamer-filling robot is proposed in this paper, as shown in Figure 3. The whole robot system consists of the mechanical structure part, the infrared vision part, and the control system part. A three-degree-of-freedom serial cylindrical type robot is designed to form the mechanical body, the infrared vision is chosen to detect the leakage of steam, and the PLC is used to form the control system of the robot. Due to limited space, the mechanical structure part of the whole robot system is the main research object in this paper.

When viewed as a whole, the exclusive steamer-filling robot proposed in this paper is a three-degree-of-freedom cylindrical robot, as shown in Figures 3 and 4. The robot can be seen as a R-P-R cylindrical type robot where, R and P stand for revolute and prismatic joints, respectively; firstly, the driving motor 1 and gearbox form a rotational motion around z-axis; thus the whole body of the robot can realize a rotational motion around the z-axis. Then the driving motor and ball screw form a translational motion along the z-axis. Finally, the driving motor 3 and gearbox form another rotational motion around z'-axis, which is parallel with the z-axis.

The working process of the exclusive steamer-filling robot is designed as follows: firstly, the fermenting grains are carried to the manipulator arm 1 though the hopper of the robot; then, these fermenting grains are transformed from point A to point B by using screw conveyors arranged in the manipulator arm 1. Next, these fermenting grains are pushed into the manipulator arm 2 at point B. Finally, by the same way, these fermenting grains are pushed out the manipulator arm 2 at point C by using screw conveyors arranged in manipulator arm 2, so as to complete the whole operation process. From the perspective of degree of freedom, the proposed steamer-filling robot has same 3-DOFs with SCARA type robots, namely, two rotational motions and one translational motion. But as far as function is concerned, the proposed steamer-filling robot is totally different from SCARA type robots, because the arms of the steamer-filling robot are used as multifunctional bodies, that is, not only used to transmit motion as robot arms but also used to carry the fermenting grains as actuating mechanism, that is, a noticeable difference between the proposed steamer-filling robot and SCARA type robots.

Furthermore, compared with existing steamer-filling robot, this type of robot can fill fermenting grains in a continuous mode without being standstill in the operation process, which is of great importance regarding liquor yield and liquor quality.

3. Kinematics Problem Analyses of the Robot

In this section, the kinematics problems in terms of position analysis, workspace, and dexterity of the robot are analyzed in detail [5–11]. First, the inverse and the forward positon analyses of the mechanism are calculated by explicit solution; then the workspace of the robot is determined based on the forward position analysis algorithm. Finally, the dexterity and the transmission performance of the manipulator are carried out by the conception of transmission angles.

3.1. Position Analysis. In order to increase liquor-making efficiency, one steamer-filling robot fills fermenting grains into two fermentation containers as shown in Figure 5. For analysis purpose, a plane coordinate system Axy is founded. Point A is coordinate origin; points O_1, O_2 are the center points of two fermentation containers, setting x-axis parallel to line O_1O_2; and two fermentation containers are

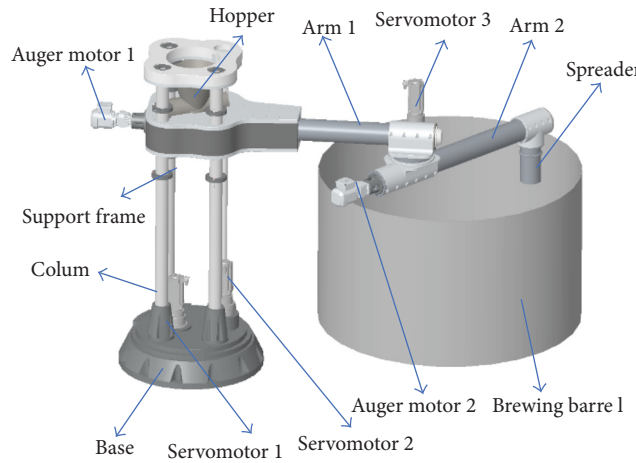

Figure 3: CAD model of the robot.

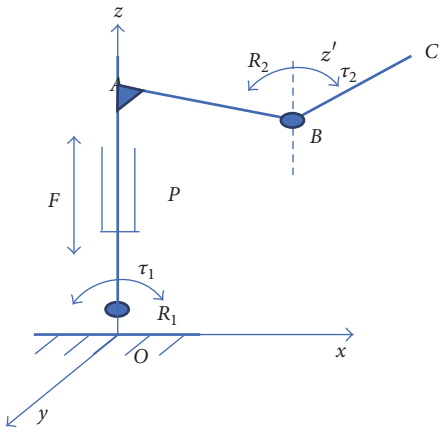

Figure 4: Schematic diagram of the robot.

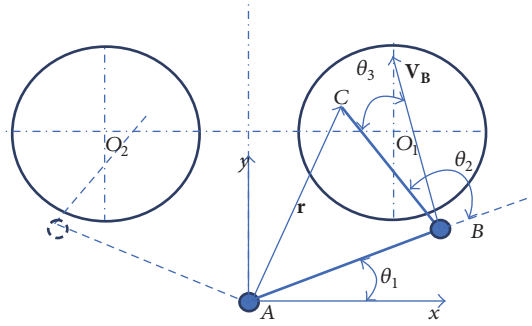

Figure 5: Schematic diagram of the robot (vertical view).

symmetrically distributed about y-axis. According to these geometric relationships, closed-loop position equation of the robot can be expressed as

$$r = \overrightarrow{AB} + \overrightarrow{BC}. \tag{1}$$

Expanding (1) yields

$$\begin{aligned} x &= l_1 \cos(\theta_1) + l_2 \cos(\theta_1 + \theta_2), \\ y &= l_1 \sin(\theta_1) + l_2 \sin(\theta_1 + \theta_2). \end{aligned} \tag{2}$$

According to (2), given a set of (θ_1, θ_2), the position coordinate (x, y) of the end of the robot can be calculated directly, which is the forward position solution of the mechanism. Here, $l_1 = \|AB\|$, $l_2 = \|BC\|$.

In order to get the inverse positon analysis of the robot, from (2), an equation about the relation between the parameters of θ_1, θ_2 and x, y can be deduced as follows:

$$(x - l_1 \cos\theta_1)^2 + (y - l_1 \sin\theta_1)^2 = l_2^2. \tag{3}$$

Expanding (3) yields

$$x^2 + y^2 + l_1^2 - l_2^2 = 2l_1 (x \cos\theta_1 + y \sin\theta_1). \tag{4}$$

In order to simplify the calculation, we assume that

$$\tan\theta = \frac{y}{x}, \quad \text{namely } \theta = \arctan\frac{y}{x}. \tag{5}$$

Substituting (5) into (4) yields

$$x^2 + y^2 + l_1^2 - l_2^2 = \frac{2l_1 x}{\cos\theta} \cos(\theta_1 \pm \theta). \tag{6}$$

According to (7), two set solutions of θ_1 and θ_2 can be expressed by the following:

$$\begin{aligned} \theta_1 &= \theta + \arccos\left(\frac{\cos(\theta)\left(x^2 + y^2 + l_1^2 - l_2^2\right)}{2l_1 x}\right), \\ \theta_2 &= \arccos\left(\frac{x - l_1 \cos(\theta_1)}{l_2}\right) - \theta_1, \end{aligned} \tag{7}$$

$$\begin{aligned} \theta_1 &= \arccos\left(\frac{\cos(\theta)\left(x^2 + y^2 + l_1^2 - l_2^2\right)}{2l_1 x}\right) - \theta, \\ \theta_2 &= \arccos\left(\frac{x - l_1 \cos(\theta_1)}{l_2}\right) - \theta_1. \end{aligned} \tag{8}$$

Table 1: Forward position analysis for the robot.

Case (a)			
Inputs		Outputs	
θ_1 (°)	θ_2 (°)	x (mm)	y (mm)
30	60	1558.8	2400

According to (7) and (8), given a set of the position coordinate (x, y) of the end of the robot, two sets of the joint locations (θ_1, θ_2) of the manipulator arm of the robot can be calculated directly, which is the inverse positon solution of the mechanism.

3.2. Jacobian Matrix and Singularity of the Robot. In order to get the Jacobian matrix of the robot, derived from both sides of (2), rewriting the equation in matrix form yields

$$\mathbf{v} = \mathbf{J}\boldsymbol{\omega}, \tag{9}$$

where $\mathbf{v}$ stands for the linear velocity of the end of the robot, $\boldsymbol{\omega}$ stands for the rotation speed of these two rotational joint, and $\mathbf{J}$ is the Jacobian matrix of the robot.

Here,

$$\mathbf{v} = \begin{bmatrix} \dot{x} \\ \dot{y} \end{bmatrix},$$

$$\boldsymbol{\omega} = \begin{bmatrix} \dot{\theta}_1 \\ \dot{\theta}_2 \end{bmatrix}, \tag{10}$$

$$\mathbf{J} = \begin{bmatrix} -l_1 \sin(\theta_1) - l_2 \sin(\theta_1 + \theta_2) & -l_2 \sin(\theta_1 + \theta_2) \\ l_1 \cos(\theta_1) + l_2 \cos(\theta_1 + \theta_2) & l_2 \cos(\theta_1 + \theta_2) \end{bmatrix}.$$

When the robot is singular,

$$\det(\mathbf{J}) = 0. \tag{11}$$

Expanding (11) gives the following result:

$$l_1 l_2 \sin(\theta_2) = 0. \tag{12}$$

From (12), when $\theta_2 = 0$ or π, namely, the two manipulator arms are collinear, the robot is singular.

Since Jacobian matrix inherently combines information about the position, orientation, and joint limits of the end-effector, the dexterity analysis of the robot can be carried out based on the Jacobian matrix, and the dexterity measure can be defined as

$$\lambda = \sqrt{\det(JJ^T)}. \tag{13}$$

3.3. Transmission Angel and Transmission Performance of the Robot. In order to evaluate the transmission performance of the mechanism, a transmission angle is designed. At a particular moment, the linear velocity of the end of the manipulator arm 1 is defined as $\mathbf{V}_B$ as shown in Figure 5; at this time, the axis of the manipulator arm 2 and the direction vector of $\mathbf{V}_B$ form an included angle θ_3. Then the angel is defined as the transmission angel θ_3 of the robot between the two manipulator arms, and the cosine value of the angel is defined as the transmission index of the two manipulator arms.

$$k = \cos(\theta_3). \tag{14}$$

Here, $k \in [0, 1]$. When $\theta_3 = 0$, $\cos(\theta_3) = 1$; this means that, in this situation, the transmission performance of the manipulator arms is best. When $\theta_3 = \pi$, $\cos(\theta_3) = 0$; this means that the two manipulator arms are collinear in this situation, the robot is in singular configuration, and this configuration is the worst situation.

4. Numerical Examples

In this section, the positon analysis, workspace, dexterity, and transmission performance of the mechanism are enumerated by corresponding numerical simulations. For consistency, the length parameters of two arms are defined as follows: $l_1 = 1800$ mm, $l_2 = 1500$ mm. The central points of fermentation containers are set as follows: $O_1 = (1390\text{ mm}, 2055\text{ mm})$, $O_2 = (-1390\text{ mm}, 2055\text{ mm})$. The swing angle ranges of the two manipulator arms are set as follows: $\theta_1 \in [-25^\circ, 230^\circ]$, $\theta_2 \in [30^\circ, 150^\circ]$.

4.1. Position Analysis Simulations. For the forward positon analysis, given one random group of inputs (θ_1, θ_2), the position coordinate (x, y) of the end of the robot can be calculated, and the corresponding parameters are listed in Table 1; meanwhile, the corresponding configurations relative to the computed solutions are described in Figure 6.

For the inverse positon analysis, given a set of the position coordinate (x, y) of the end of the robot, the joint location (θ_1, θ_2) of the manipulator arm of the robot can be calculated; the corresponding parameters are listed in Table 2; meanwhile, the corresponding configurations relative to the computed solutions are described in Figure 7.

4.2. Workspace Determination Simulations. The workspace determination of the robot can be carried out based on the forward position analysis algorithm, and a meshless method is applied to determine the reachable workspace of the robot. The reachable workspace of mechanism is shown in Figure 8.

4.3. Dexterity Analysis Simulation of the Robot. The dexterity of the robot can be thought as the ability of the manipulator to arbitrarily change its position and orientation or apply forces and torques in arbitrary directions. In this section, the dexterity of the robot can be obtained by using (13), and the simulation of the mechanism can be calculated as shown in Figure 9.

Table 2: Inverse position analysis for the robot.

Case (a)			
Inputs		Outputs	
x (mm)	y (mm)	θ_1 (°)	θ_2 (°)
1558.8	2400	30	60.0017
		83.9926	−60.0017

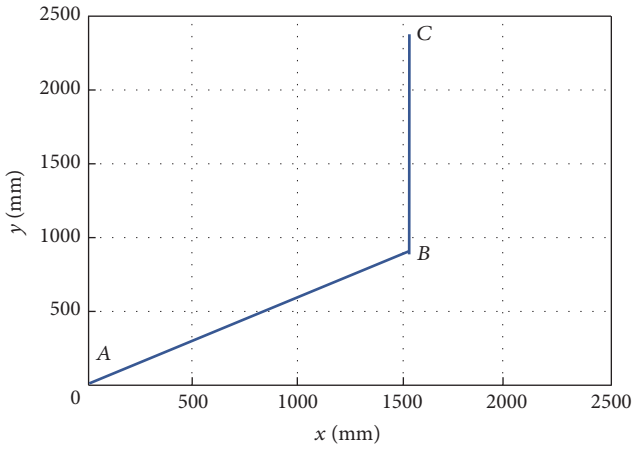

Figure 6: Different configurations for forward position.

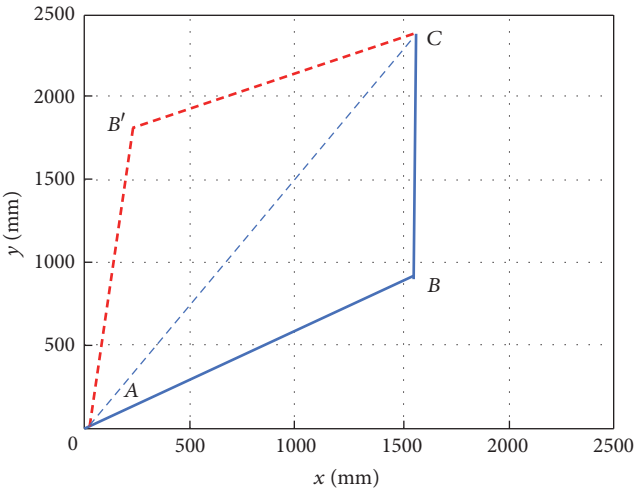

Figure 7: Different configurations for inverse position.

4.4. Transmission Performance of the Robot. Transmission performance of the robot will be carried out through the pressure angles between two arms. The transmission performance of the robot can be obtained based on (14), and the solutions are described in Figures 10 and 11.

5. Dynamics Analysis of the Robot

In this section, the dynamics analysis of the robot is carried out on the base of the kinematics modeling and Lagrange dynamics equation.

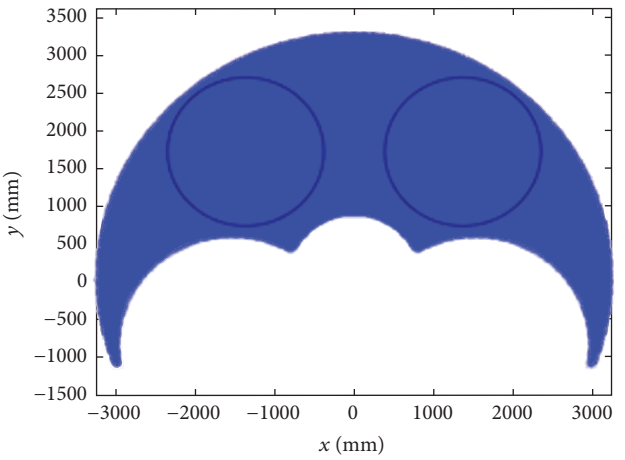

Figure 8: The reachable workspace of the mechanism.

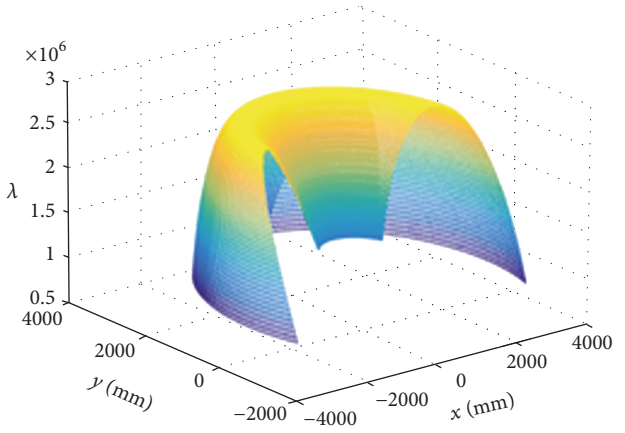

Figure 9: The dexterity analysis simulation of the robot.

According to the dynamic model of multilink mechanism, the dynamic equation of the robot can be founded:

$$\boldsymbol{\tau} = \mathbf{H}(\mathbf{q})\,\ddot{\mathbf{q}} + \mathbf{C}(\mathbf{q}\ \ \dot{\mathbf{q}})\,\dot{\mathbf{q}} + \mathbf{G}(\mathbf{q}), \tag{15}$$

where $\boldsymbol{\tau}$ stands for the joint drive torque of robot, $\mathbf{q}$, $\dot{\mathbf{q}}$, $\ddot{\mathbf{q}}$ stand for position, velocity, and acceleration vectors of robot joints, $\mathbf{H}(\mathbf{q})$, $\mathbf{C}(\mathbf{q}\ \ \dot{\mathbf{q}})$, $\mathbf{G}(\mathbf{q})$ represent inertial matrix, Coriolis force and centripetal force matrix, and gravity matrix of the manipulator, respectively.

As shown in Figure 4, It should be noted that the force $\mathbf{F}$ along the z-axis can be calculated directly by mechanical formula:

$$\mathbf{F} = m\mathbf{g} + m\mathbf{a}, \tag{16}$$

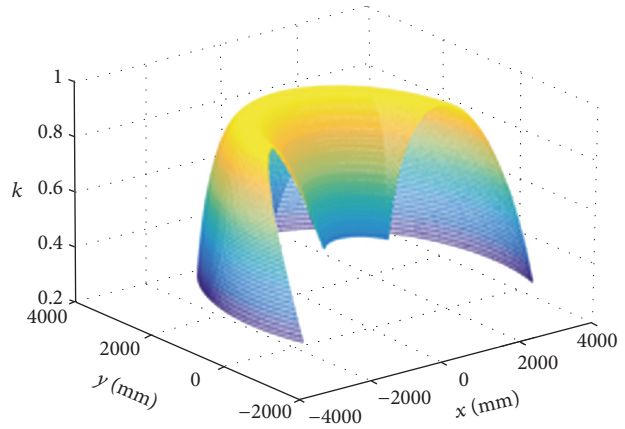

Figure 10: Transmission performance of the robot.

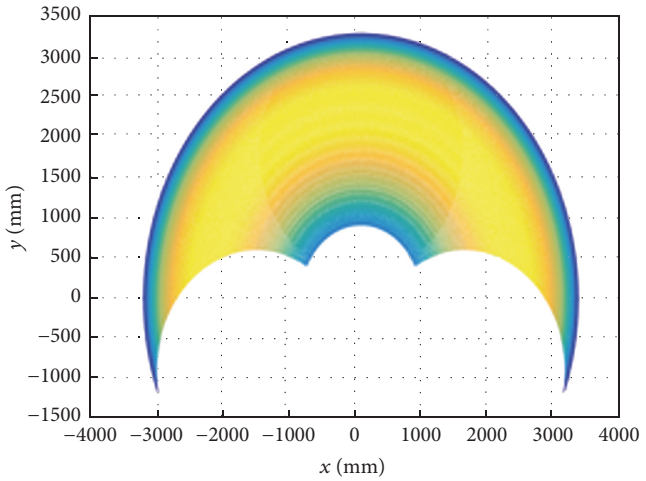

Figure 11: Transmission performance of the robot in x-y plane.

where m is the all weight of robot arm including fermenting grains and **g** and **a** are gravitational acceleration and translational motion acceleration of robot arm along the z-axis.

The drive torques of two revolute joints can be calculated by Lagrange dynamics equation:

$$\begin{bmatrix} \tau_1 \\ \tau_2 \end{bmatrix} = \begin{bmatrix} H_{11} & H_{12} \\ H_{21} & H_{21} \end{bmatrix} \begin{bmatrix} \ddot{q}_1 \\ \ddot{q}_2 \end{bmatrix} + \begin{bmatrix} C_{11} & C_{12} \\ C_{21} & C_{21} \end{bmatrix} \begin{bmatrix} \dot{q}_1 \\ \dot{q}_2 \end{bmatrix}, \quad (17)$$

where

$$\begin{aligned} H_{11} &= I_{z1} + I_{z2} + m_1 x_1^2 + m_2 \left(l_1^2 + x_2^2\right) \\ &\quad + 2 l_1 x_2 m_2 \cos\left(\theta_2\right), \\ H_{12} &= I_{z2} + m_2 x_2^2 + l_1 x_2 m_2 \cos\left(\theta_2\right), \\ H_{21} &= H_{12}, \\ H_{22} &= I_{z2} + m_2 x_2^2, \\ C_{11} &= -2\dot{\theta}_2 \sin\left(\theta_2\right) l_1 x_2 m_2, \end{aligned}$$

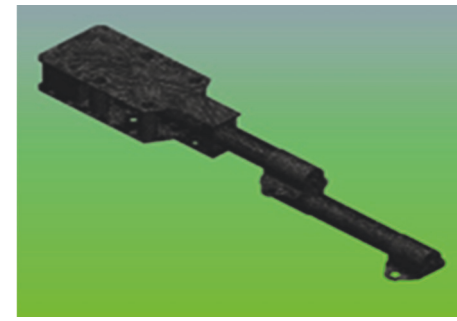

Figure 12: Finite element analysis model of steamer-filling robot.

$$\begin{aligned} C_{22} &= 0, \\ C_{21} &= \dot{\theta}_1 \sin\left(\theta_2\right) l_1 x_2 m_2, \end{aligned} \quad (18)$$

where m_1 and m_2 stand for the weights of arm 1 and arm 2 including fermenting grains, l_1 and l_2 stand for the lengths of arm 1 and arm 2, and x_1 and x_2 stand for the gravity center positions of arm 1 and arm 2.

For the inverse dynamic analysis, the drive torques of two revolute joints, and the drive force of the translate joint can be calculated by (16) and (17), given the position, velocity, acceleration, weights, and dimensional parameters of the robot. For the forward dynamic analysis, the weights of fermenting grains can be obtained by (16) and (17), given the position, velocity, acceleration, dimensional parameters, and drive forces of the robot.

6. Static Stiffness Analysis of the Robot

Taking into consideration the high positioning accuracy and slow rate requirements of work situation for the steamer-filling robot, the static stiffness analysis of the robot is studied by means of finite element method in this section. First, according to the original geometric model, a finite element analysis model was established using commercial software, as shown in Figure 12. Then, the actual working constraint conditions are given to the finite element analysis model. Finally, the static stiffness of the robot in different working positon is calculated by software, and the results are shown in Figures 13 and 14.

7. Experimental Results

The physical prototype of the steamer-filling robot is shown in Figures 15 and 16, which is used in the distillery. According to the production data comparison, liquor output was about 210 KG from 500 KG fermenting grains by using the steamer-filling robot, compared with about 190 KG by manual process, and the robot method has a wide application prospect.

8. Conclusions

The major contribution of this research is proposing a novel exclusive steamer-filling robot, compared with existing

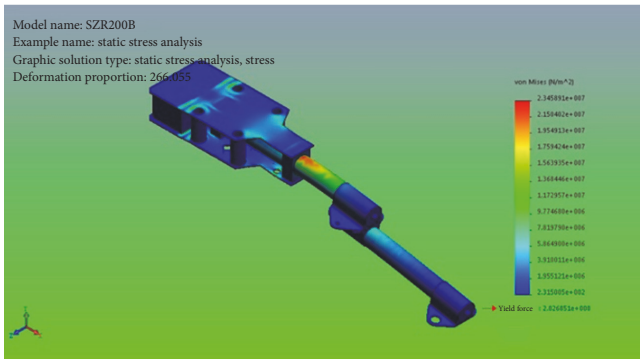

Figure 13: Finite element stress analysis of the robot.

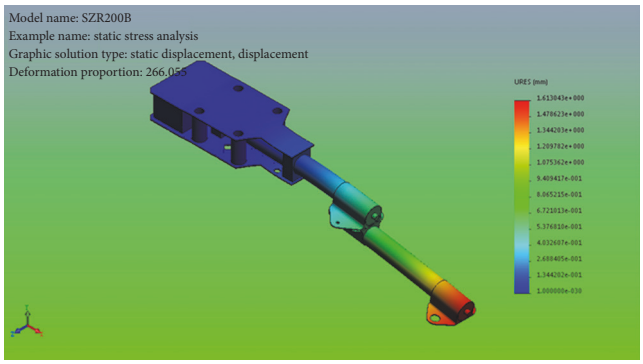

Figure 14: Finite element displacement analysis of the robot.

Figure 15: Experimental prototype of steamer-filling robot.

Figure 16: Steamer-filling robot used in field.

steamer-filling robot; this type robot can fill fermenting grains in a continuous mode without being standstill in the operation process, which is of great importance to liquor yield and liquor quality. Firstly, the steamer-filling operation process is described, and the structure composition and function realization of the robot are particularly introduced. Secondly, the kinematics problems in terms of position analysis, workspace analysis, dexterity analysis, and transmission performance of the robot are analyzed. Thirdly, experimental analyses are made to prove the validity and efficiency of the robot system. On the basis of the kinematics study of the robot, the inverse and forward dynamics analysis and stiffness performance and kinematic optimization of the robot will be investigated in future work, and the application and spread of this novel steamer-filling robot is of vital significance to the liquor-making industry.

Conflicts of Interest

The authors declare that there are no conflicts of interest regarding the publication of this paper.

Acknowledgments

This work was supported by Intelligent Manufacturing Technology Major Project of Tianjin (15ZXZNGX00040, 15ZXZNGX00270, and 16ZXZNGX00070).

References

[1] B. Li, Y. Li, and X. Zhao, "Kinematics analysis of a novel over-constrained three degree-of-freedom spatial parallel manipulator," *Mechanism and Machine Theory*, vol. 104, pp. 222–233, 2016.

[2] B. Li, Y. M. Li, X. H. Zhao, and W. M. Ge, "Kinematic analysis of a novel 3-CRU translational parallel mechanism," *Mechanical Sciences*, vol. 6, no. 1, pp. 57–64, 2015.

[3] Q. Yan, B. Li, Y. Li, and X. Zhao, "Comparative study of two 2-RPU+SPR parallel manipulators," in *Proceedings of the 12th World Congress on Intelligent Control and Automation, WCICA 2016*, pp. 1975–1980, chn, June 2016.

[4] Y. Li and Q. Xu, "Kinematic analysis of a 3-PRS parallel manipulator," *Robotics and Computer-Integrated Manufacturing*, vol. 23, no. 4, pp. 395–408, 2007.

[5] X.-J. Liu, X. Tang, and J. Wang, "HANA: A novel spatial parallel manipulator with one rotational and two translational degrees of freedom," *Robotica*, vol. 23, no. 2, pp. 257–270, 2005.

[6] J. Wang and X.-J. Liu, "Analysis of a novel cylindrical 3-DoF parallel robot," *Robotics and Autonomous Systems*, vol. 42, no. 1, pp. 31–46, 2003.

[7] B. Bihari, D. Kumar, C. Jha, V. S. Rathore, and A. K. Dash, "A geometric approach for the workspace analysis of two symmetric planar parallel manipulators," *Robotica*, vol. 34, no. 4, pp. 738–763, 2016.

[8] D. Sen and B. N. Singh, "A geometric approach for determining inner and exterior boundaries of workspaces of planar manipulators," *Journal of Mechanical Design*, vol. 130, no. 2, Article ID 022306, 2008.

[9] S. Yahya, M. Moghavvemi, and H. A. F. Mohamed, "Geometrical approach of planar hyper-redundant manipulators:

Inverse kinematics, path planning and workspace," *Simulation Modelling Practice and Theory*, vol. 19, no. 1, pp. 406–422, 2011.

[10] M. Gallant and R. Boudreau, "The synthesis of planar parallel manipulators with prismatic joints for an optimal, singularity-free workspace," *Journal of Robotic Systems*, vol. 19, no. 1, pp. 13–24, 2002.

[11] A. M. Hay and J. A. Snyman, "The determination of nonconvex workspaces of generally constrained planar Stewart platforms," *Computers & Mathematics with Applications*, vol. 40, no. 2000, pp. 1043–1060, 2000.